King Saud University

Arabian Journal of Chemistry

www.ksu.edu.sa
www.sciencedirect.com

ORIGINAL ARTICLE

The simultaneous elimination of arsenic and mercury ions via hollow fiber supported liquid membrane and their reaction mechanisms: Experimental and modeling based on DFT and generating function

Sira Suren [a], Wikorn Punyain [b], Kreangkrai Maneeintr [c], Kasidit Nootong [a], Ura Pancharoen [a],*

[a] *Department of Chemical Engineering, Faculty of Engineering, Chulalongkorn University, Bangkok 10330, Thailand*
[b] *Department of Chemistry and NU-Research Center for Petroleum, Petrochemicals and Advanced Materials, Faculty of Science, Naresuan University, Phitsanulok 65000, Thailand*
[c] *Department of Mining and Petroleum Engineering, Faculty of Engineering, Chulalongkorn University, Bangkok 10330, Thailand*

Abstract This study investigates the simultaneous removal of low concentrations of arsenic and mercury ions from synthetic produced water via hollow fiber supported liquid membrane (HFSLM). Results show that HFSLM can remove both arsenic and mercury ions from synthetic produced water to less than 0.02 and 0.001 mg·L^{-1}, respectively. These final concentrations comply with the wastewater standard of Thailand. Percentages of extraction for arsenic and mercury ions proved to be about 100 %. Those of recovery for arsenic and mercury ions reached 70 % and 75 %, respectively. A quantum model based on density functional theory (DFT) is introduced to analyze the forming and breaking of supramolecular complex species in the processes of extraction and recovery, respectively. Furthermore, the concept of Generating Function is applied to construct a mathematical model for forecasting the potential of removing metal ions via HFSLM. The mathematical model conforms to the experimental data, having an average relative deviation of 5 %. The

* Corresponding author.
  E-mail address: ura.p@chula.ac.th (U. Pancharoen).

Production and hosting by Elsevier
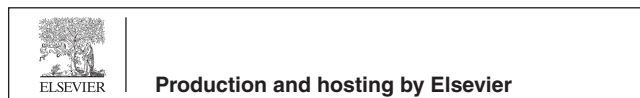
Nomenclature

$C_{A,F}$	concentration of metal ions in the feed phase (mg·L^{-1})
$C_{A,F}(x_i)$	concentration of metal ions in the outlet feed solution (mg·L^{-1})
$C_{A,F}(x_0)$	concentration of metal ions in the inlet feed solution (mg·L^{-1})
$C_{A,S}$	concentration of metal ions in the strippant phase (mg·L^{-1})
$C_{A,S}\left(\hat{x}_i'\right)$	concentration of metal ions in the outlet stripping solution (mg·L^{-1})
$C_{Expt.}$	concentration of metal ions attained from the experiment (mg·L^{-1})
C_{Model}	concentration of metal ions attained from the mathematical model (mg·L^{-1})
D_A	distribution coefficient of recovery utilizing the single substance A (-)
D_B	distribution coefficient of recovery utilizing the single substance B (-)
D_{max}	optimum distribution coefficient of the synergistic system (utilizing a combination of the reactants A and B) (-)
$E_C[\rho(r)]$	electron–electron correlation energy (J)
$E_X[\rho(r)]$	exchange energy (J)
$E_{XC}[\rho(r)]$	exchange–correlation energy (J)
$E[\rho(r)]$	energy of all specific energy parts (J)
i	number of increments (-)
k_{Ex}	reaction rate constant of extraction
k_{Re}	reaction rate constant of recovery
L	hollow fiber's effective length (dm)
m	reaction order of extraction (-)
N	number of observations (-)
n	reaction order of recovery (-)
q_F	volumetric flow rate of the aqueous feed solution (L·s^{-1})
R	synergistic coefficient (-)
r_i	internal radius of the hollow fiber (dm)
$r_{A,Ex}$	reaction rate of extraction
$r_{As,Re}$	reaction rate of recovery
t	time (s)
$T_{ni}[\rho(r)]$	kinetic energy of the non-interacting electron (J)
$\Delta T[\rho(r)]$	correction to the kinetic energy (J)
V_F	volume of an increment of the hollow fiber (L)
$V_{ee}[\rho(r)]$	classical electron–electron repulsion energy (J)
$V_{ne}[\rho(r)]$	nuclear-electron interaction energy (J)
$\Delta V_{ee}[\rho(r)]$	all non-classical correction to the electron–electron repulsion energy (J)
x	longitudinal axis of the hollow fiber in the feed phase (dm)
$\hat{x}'$	longitudinal axis of the hollow fiber in the strippant phase (dm)
Δx	increment of the hollow fibers divided (dm)
$\rho(r)$	electron density (e$^-$·Å^{-3})
ε_{XC}	energy density (J·L^{-1}).

results of this study provide a better understanding of the transport mechanisms of arsenic and mercury ions.

1. Introduction

Offshore oil and gas production generate produced water, which is usually polluted with arsenic and mercury (Gallup and Strong, 2007; Neff et al., 1987). Both arsenic and mercury are highly poisonous metals that can cause chronic or acute poisoning in humans depending on the amount taken (Pajuelo et al., 2008; Van der Vaart et al., 2001). The quantity of these poisonous metals released into the environment is increasing in accordance with the increase in the amount of wastewater generated by the offshore oil and gas sectors, together with other sites such as petroleum refineries and the metallurgical industry (Sun et al., 2021). Arsenic and mercury concentrations in various wells range from 1 to 4 mg·L^{-1} (Lothongkum et al., 2011; Pancharoen et al., 2009; Pancharoen et al., 2010) and from 0.5 to 1 mg·L^{-1} (Lothongkum et al., 2011; Pancharoen et al., 2010). Toxic metals released into the environment can accumulate and can affect food safety, which is currently a significant issue for human life and health (Hu et al., 2021). As a result, Thailand's Ministries of Industry and Natural Resources and Environment have both mandated that arsenic and mercury levels in

effluents must not exceed 0.25 and 0.005 mg·L^{-1}, respectively (Thailand regulatory discharge standards, 1996).

Adsorption, ion exchange, coagulation, oxidation, together with precipitation have traditionally been used in the removal of hazardous metals from produced water. Nonetheless, even after such treatment, the amount of arsenic and mercury in the produced water is found to be greater than the wastewater discharge standard (Gallup and Strong, 2007). These techniques also have some disadvantages. Inbaraj et al. (2009) have reported that the application of these techniques is inadequate when the concentration of the target ions is as low as µg·L^{-1} level. Adsorbents pose a huge challenge in the selective separation of chemical compounds (Li et al., 2021). Various adsorbents, including SiO$_2$-NH$_2$, activated carbons, and activate aluminum oxide, suffer from limited adsorption efficiency (Liu et al., 2020a). Meanwhile, the process of oxidation has some drawbacks due to the high quantity of oxidizing agents required (Liu et al., 2020b), the problem of corrosion behavior, the difficulty of implementation, as well as high-cost (Ge et al., 2019).

In response, produced water generated from offshore oil and gas production that exceeds discharge restrictions with

hazardous metals is re-injected into the geological formations from which the oil and gas originated (Gallup and Strong, 2007). It is seen that such an approach is unreliable since hazardous metals might leak into the environment. As a result, an alternate potential technique is necessary.

Hollow fiber supported liquid membrane (HFSLM) is acknowledged to be a promising technique for the removal of low concentrations of target ions ($\mu g \cdot L^{-1}$ levels) from a variety of solutions (Güell et al., 2008; Scott et al., 2020). HFSLM is seen to be more beneficial than conventional approaches, providing higher selectivity (Sunsandee et al., 2017; Sunsandee et al., 2018) but requiring lower extractant (carrier), less solvent, less energy as well as less capital and operating costs (San Román et al., 2010). HFSLM's large surface area allows for a rapid rate of mass transfer of separation (Kocherginsky et al., 2007). HFSLM is also useful in a variety of sectors such as treatment of wastewater (Güell et al., 2008; Rathore et al., 2001), food along with biological processing (Kocherginsky et al., 2007; Lipnizki, 2010), and pharmaceuticals (Sunsandee et al., 2017).

Previously, HFSLM has been used to remove arsenic (Pancharoen et al., 2009) and/or mercury ions (Pancharoen et al., 2010). However, no study has succeeded in the simultaneous separation of arsenic and mercury ions in a single-step operation. Therefore, the findings from previous studies are not suitable to apply in the treatment of wastewater generated from offshore oil and gas production. In this work, the removal of both arsenic and mercury ions in a single-step operation is of pivotal importance.

The efficacy of removal of target ions via HFSLM is dependent on various parameters: the chemical composition of the solution, the concentration of solute, the type of organic carriers as well as strippants utilized, the acidity of the bulk solution, and flow velocity (Bai et al., 2019). As a result, such factors have been investigated in this study.

To improve and forecast metal ion extraction and stripping, an understanding of the mechanisms of metal ion extraction and stripping is required. However, investigations into the mechanisms of metal ion extraction and stripping reactions, particularly those involving arsenic and mercury ions, are sparse. Thus, the molecular structural chemistry of complex species arising due to reactions is a significant factor in determining the mechanisms of extraction and stripping reactions of metal ions. It is accepted that density functional theory (DFT) is an effective quantum–mechanical approach for analyzing the intermolecular chemistry of the reactions (Van Mourik et al., 2014). Moreover, DFT can estimate the energy and bond length of the molecules (Nasim Rahnama et al., 2021).

In order to describe the phenomena of mass transport within HFSLM, a mathematical model is required. A mathematical model is essential in scaling up the HFSLM system for use in the treatment of a higher volume of wastewater, especially wastewater from the oil and gas industries. A mathematical model can also be utilized for forecasting the effectiveness of wastewater treatment. For these reasons, researchers have developed mathematical models for the removal of metal ions through HFSLM. Such models have been created based on the characteristics of systems such as flow patterns (circulating flow or continuous flow), predominant factors of the transport of target ions (convection, diffu-

sion, or reaction), and conditions of the system: transition state (Chaturabul et al., 2012; Choi et al., 2001; Kamran Haghighi et al., 2019; Mishra et al., 2021; Pancharoen et al., 2011), pseudo-steady-state (Kandwal et al., 2011), or steady-state (Zhang et al., 2010). Most of the models have been considered at the transition state, though not all systems are at the transition state. Hence, it is necessary to develop a mathematical model, which can forecast the removal of target ions at a steady-state condition.

This study examines the treatment of synthetic wastewater containing a relatively low concentration of arsenic and mercury ions using HFSLM. The crucial factors studied consist of the types and concentration of the organic carriers, acidity of feed solution, types and concentration of the strippant solutions, as well as flow rates of feed and strippant solutions. Further, the stability of the HFSLM system is investigated. DFT is introduced to describe the mechanisms of extraction and stripping of arsenic and mercury ions. Finally, a Generating Function was applied to create a mathematical model to forecast the efficacy of extraction at a steady-state condition.

2. Experimental

2.1. Chemicals

Deionized water was utilized to prepare aqueous solutions (feed and stripping solutions). Both arsenic acid (H_3AsO_4) and mercury(II) chloride ($HgCl_2$) were used to prepare the synthetic wastewater as feed solution. The initial pH of feed solution was 6 and the initial concentrations of H_3AsO_4 and $HgCl_2$ were 1 and 4 $mg \cdot L^{-1}$, respectively. Such conditions were carried out to simulate the condition of the produced water obtained from the offshore oil and gas production in the Gulf of Thailand (Lothongkum et al., 2011; Pancharoen et al., 2010). Sodium hydroxide (NaOH) and hydrochloric acid (HCl) were employed to adjust the acidity of the feed solution and investigate various types of strippant solutions. Four effective carriers observed from previous studies; namely, Aliquat 336 (Fábrega and Mansur, 2007; Pancharoen et al., 2009), Trioctyl amine (TOA) (Pancharoen et al., 2010), Tributyl phosphate (TBP) (Jantunen et al., 2019), and Trioctylphosphine oxide (Cyanex 921) (Perez et al., 2007)) were chosen to determine the most suitable carrier for the extraction of both arsenic and mercury ions. Toluene was utilized to dilute the organic carriers. All reagents were of AR grade and utilized without additional purification.

2.2. Apparatus

The hollow fiber module comprising 35,000 microporous polypropylene fibers was employed in the removal of arsenic and mercury ions. Table 1 depicts the features of the hollow fiber module utilized. Two gear pumps were implemented for pumping both feed and stripping solutions into the hollow fiber system. Fig. 1 depicts the HFSLM system as well as other equipment used. An atomic absorption spectrometer (AAS) (model AA240FS), which has a detection limit of 0.001 $mg \cdot L^{-1}$ and a deviation of 0.9995, was utilized to evaluate the concentration of metal ions. The pH meter (model

Table 1 Features of the hollow fiber module (3M^{TM} Liqui-Cel^{TM} EXF Series Membrane Contactor).

Features	Details
Module diameter (dm)	0.63
Effective length of hollow fiber (dm)	2.03
Number of hollow fibers (-)	35,000
Inside radius of hollow fiber (dm)	1.2×10^{-3}
Outside radius of hollow fiber (dm)	1.5×10^{-3}
Contact area (dm^2)	1.4×10^{-6}
Area per unit volume (dm^{-3})	2.93×10^{-2}
Pore size (dm)	3×10^{-7}
Tortuosity	2.6
Porosity (%)	25
Material	Polypropylene

EUTECH pH 700) was utilized to measure the acidity of the feed solution.

2.3. Procedure

Four effective carriers (Aliquat 336, TOA, TBP, and Cyanex 921) were applied to determine their potential to extract arsenic and mercury ions simultaneously using Liquid-Liquid Extraction (LLE). Such carriers were diluted with toluene and utilized at an excess concentration of 0.68 M. The most potential carrier was applied in the HFSLM process.

In the HFSLM process (see Fig. 1), the chosen carrier diluted with toluene as the liquid membrane was cycled along the tube and shell sides of the hollow fibers concurrently until 0.052 L of the liquid membrane was used. This volume relates to the total volume of hollow-fiber micropores. The excess liquid membrane was then purged by passing deionized water through the tube and shell sides of the hollow fibers. Next, both feed solution (synthetic produced water) and strippant solution were fed counter-currently into the hollow fibers' tube and shell sides. Flow patterns of both feed and strippant solutions were single pass. Finally, 0.02 L for each of the outlet feed and strippant solutions was collected to evaluate the concentration of metal ions using AAS.

The concentration of the chosen carrier, pH of the feed solution, types of strippant solutions used, the concentration of the chosen strippant solution as well as operation time were varied. After each experiment, the liquid membrane was eliminated from the system by allowing the surfactant to flow into the hollow fibers' tube and shell sides. Subsequently, deionized water was pumped into the hollow fibers to remove the surfactant.

The efficiency of extraction and recovery is defined as in Eqs. (1) and (2), respectively:

$$\%\text{Extraction} = \left[\frac{\mathscr{C}_{A,F}(x_0) - \mathscr{C}_{A,F}(x_i)}{\mathscr{C}_{A,F}(x_i)}\right] \times 100 \tag{1}$$

$$\%\text{Recovery} = \left[\frac{C_{A,S}\left(\hat{x}_i^{A'}\right)}{\mathscr{C}_{A,F}(x_0) - \mathscr{C}_{A,F}(x_i)}\right] \times 100 \tag{2}$$

where $C_{A,F}(x_0)$ is the concentration of metal ions in the inlet feed solution (mg·L^{-1}) and $C_{A,S}\left(\hat{x}_i^{A'}\right)$ represents the concentration of metal ions in the outlet stripping solution (mg·L^{-1}).
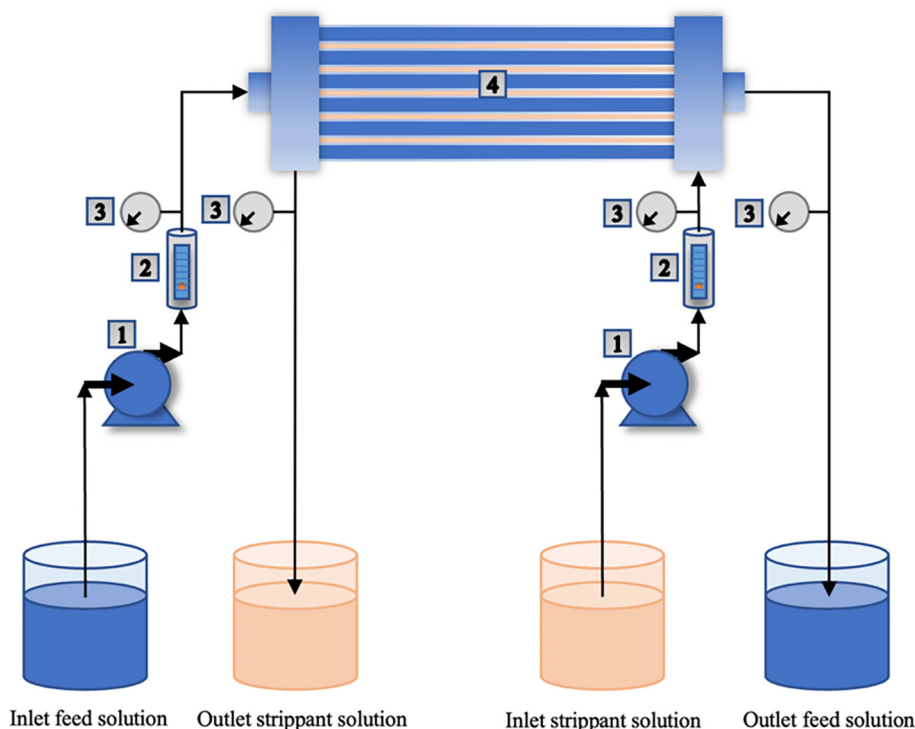

Fig. 1 Schema for the removal of arsenic and mercury ions via HFSLM: (1) gear pumps, (2) flow meters, (3) pressure gauges, and (4) hollow fiber module.

3. Results and discussion

3.1. Optimum conditions for the extraction and stripping of arsenic and mercury ions

3.1.1. Types of carriers

The neutral carriers viz. TBP (Jantunen et al., 2019) and Cyanex 921 (Perez et al., 2007) are seen as promising carriers for arsenic ions, whilst basic carriers including Aliquat 336 and TOA are seen as being effective carriers for the extraction of mercury ions (Fábrega and Mansur, 2007; Pancharoen et al., 2010). Hence, such carriers were employed in this study to determine the highest potential carrier for the simultaneous extraction of arsenic and mercury ions. In Fig. 2, results are illustrated. Thus, it is noted that Aliquat 336 had the highest potential for the simultaneous extraction of arsenic and mercury ions, resulting from the utilization of pH 6 of feed solution whereby arsenic(V) occurs mostly as dissociated species (anions) (Wilson et al., 2004). Aliquat 336 is an ionic liquid, which can extract metal ions in a variety of species (neutral and anion), although it interacts considerably better with anions.

In the case of mercury, Aliquat 336 showed the highest efficiency of mercury extraction as it is a quaternary amine, which reacts with metal ions better than TOA, a ternary amine. Aliquat 336 reacted with Hg(II) via the mechanism of ion exchange. To effectively extract mercury ions using a ternary amine like TOA, the feed solution and/or liquid membrane need(s) the addition of HCl to transform mercury ions into $HgCl_4^{2-}$ as well as to transform the ternary amine into an anion exchanger (amine salt), which is equivalent to quaternary amines (Chapman, 1997). However, the pH of the initial feed solution in this study was 6 and no HCl was added in the feed or liquid membrane phase. Therefore, TOA revealed its low efficiency in the extraction. For evaluation of other factors, Aliquat 336 diluted in toluene was utilized as the liquid membrane.

3.1.2. Concentration of chosen carrier

In Fig. 3, the impact of concentration of Aliquat 336 on the extraction and recovery of arsenic as well as mercury ions is depicted. It is seen that as the concentration of Aliquat 336 increased, so did the extractability of arsenic ions. Such a result
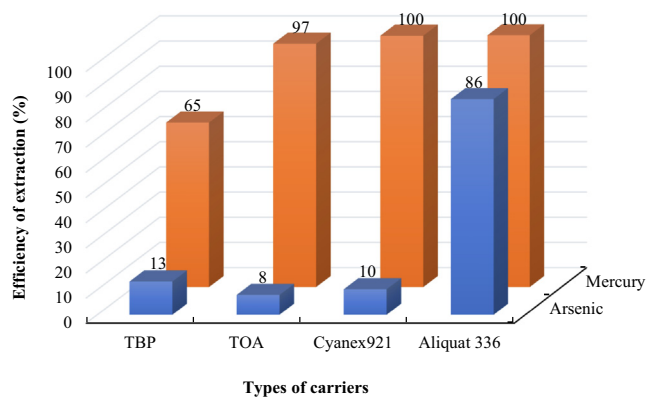
is consistent with Le Chatelier's principle, according to which higher reactant concentration leads to greater reaction. Extractability reached maximum at 0.88 M Aliquat 336. Once Aliquat 336 concentration passed over 0.88 M, no change in the efficiency of extraction was observed. In the case of mercury ions, the percentage of extraction remained constant at ∼ 100 % throughout the range of Aliquat 336 concentration investigated. Therefore, 0.88 M Aliquat 336 was used for further experiments.

3.1.3. pH of feed solution

It is well known that arsenic species in solution varies according to the acidity of the solution. As(V) occurs mostly as undissociated H_3AsO_4 at pH 2 and primarily exists as dissociated $H_2AsO_4^-$, $HAsO_4^{2-}$, and AsO_4^{3-} in pH ranges of 3 to 6, 8 to 11, and 12 to 14, respectively (Ma et al., 2018). In Fig. 4, results show that extraction of arsenic ions rose as the pH of the feed solution increased; extraction remained unchanged at pH ranging from 11 to 13. This outcome was due to Aliquat 336′s process of extraction, which involved an ion exchange of anion metal ions and Cl^- (Fontàs et al., 2000). When the pH of feed solution increases, undissociated H_3AsO_4 converts to anions and exists mostly as $HAsO_4^{2-}$ at pH 11 and as AsO_4^{3-} at pH ranging from 12 to 13 (Wilson et al., 2004), thus contributing to greater arsenic extractability as the pH of the feed solution rises. At pH levels between 11 and 13, the highest extraction of arsenic (99.6 %) was obtained, showing that Aliquat 336 extracted the dissociated species $HAsO_4^{2-}$ and AsO_4^{3-}-considerably better than $H_2AsO_4^-$. As for mercury extraction, the acidity of the feed solution did not affect the efficiency of mercury extraction; its efficiency remained constant at around 100 % over pH ranging from 2 to 13. For further investigation, the pH of the feed solution of 11 was employed.

3.1.4. Types of strippants

The most potential strippant solutions for recovery of both arsenic and mercury ions were investigated using thiourea, NaOH, and HCl (0.5 M each). NaOH is commonly used as
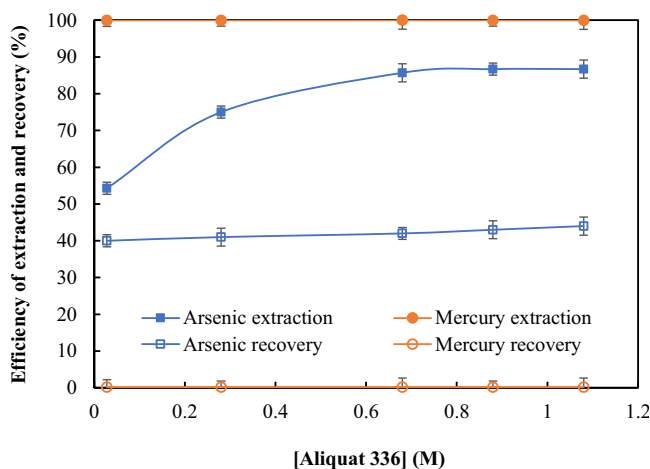

Fig. 2 Efficiency of extraction of arsenic and mercury ions using various types of carriers (0.68 M each): pH of feed solution = 6.

Fig. 3 Efficiency of extraction and recovery at various concentrations of Aliquat 336: pH of feed solution = 6, strippant solution = 0.5 M NaOH, flow rate of feed and strippant solutions = 1.67×10^{-3} L·s^{-1}, and operation time = 600 s.
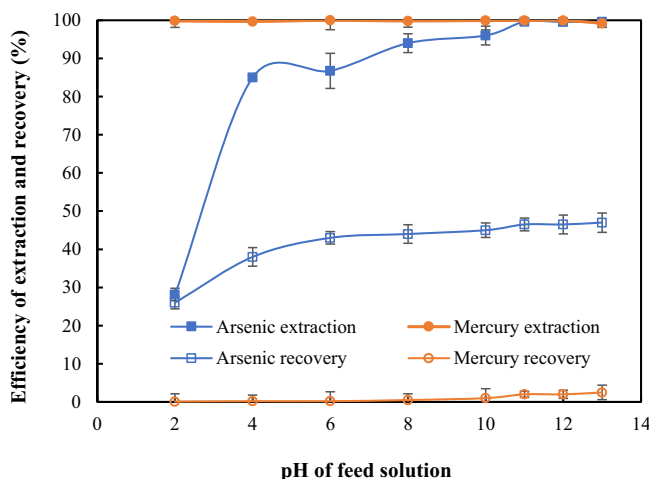
Fig. 4 Efficiency of extraction against pH of feed solution: [Aliquat 336] = 0.88 M, strippant solution = 0.5 M NaOH, flow rate of feed and strippant solutions = 1.67×10^{-3} L·s^{-1}, and operation time = 600 s.

a strippant and has been reported to have the potential for the recovery of arsenic ions (Pancharoen et al., 2009). Thiourea is noted as the favorable strippant for the recovery of target ions from metal-Ailquat 336 complex species (Fábrega and Mansur, 2007). In some cases, the mixture of thiourea and HCl as a synergistic strippant increases the potency of recovery of metal ions. This mixture has been widely used for recovering a variety of metal ions (Mohdee et al., 2021). As shown in Fig. 5, HCl proved to be the most promising strippant for arsenic ions. In contrast, the performance of thiourea and NaOH was quite poor. The low efficiency of recovery of arsenic ions utilizing NaOH and thiourea can be accounted for by the fact that once arsenic ions are stripped into such strippant solutions, they exist as anions, which can subsequently be extracted back by Aliquat 336. The recovery of arsenic and mercury ions using HCl was found to be 71 % and 29 %, respectively. When HCl was mixed with thiourea, the recovery of arsenic and mercury ions reached 82 % and
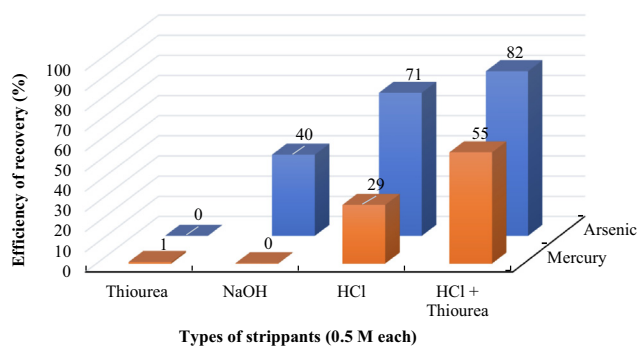
55 %, respectively. This outcome was expected owing to the synergistic effect (Luo et al., 2004). To verify such an effect, the distribution coefficients (D) of recovery, utilizing each strippant, were determined to calculate the synergistic coefficient R, as defined in Eq. (3):

$$R = \frac{D_{max}}{D_A + D_B} \qquad (3)$$

where D_{max} represents the optimum distribution coefficient of the synergistic system (utilizing a combination of the reactants A and B) to recover the metal ions. D_A refers to the distribution coefficient of recovery utilizing the single substance A, and D_B is the distribution coefficient of recovery utilizing the single substance B. If R > 1, the synergistic recovery is verified; thus, the higher the synergistic coefficient of the synergistic system, the higher the recovery.

In Fig. 6, distribution coefficients of recovery of arsenic and mercury ions are presented. Employing Eq. (3), the synergistic coefficients of recovery of arsenic and mercury ions proved to be 1.15 and 1.85, respectively, verifying the synergistic effect of the HCl/thiourea mixture. As a result, this mixture was applied as the strippant solution and their appropriate concentrations were further determined.

3.1.5. Concentrations of strippants

Fig. 7(a) and (b) depict the recovery of arsenic and mercury ions against the concentrations of HCl and thiourea. In Fig. 7(a), the recovery of metal ions utilizing 0.5 M thiourea at different concentrations of HCl is shown. Results demonstrate that the recovery of metal ions improved when the concentration of HCl increased, corresponding to chemical kinetics. The recovery of metal ions reached maximum at 0.5 M HCl. After that, the recovery of metal ions decreased due to concentration polarization, obstructing the recovery of the metal ions (Chaturabul et al., 2015; Wannachod et al., 2014).

In Fig. 7(b), the recovery of metal ions utilizing 0.5 M HCl with different thiourea concentrations is illustrated. Recovery of metal ions increased as the concentration of thiourea rose, in agreement with chemical kinetics. For recovery of arsenic ions, its optimum condition was observed at 0.5 M thiourea. After that, recovery of arsenic ions decreased due to concentration polarization (Chaturabul et al., 2015; Wannachod et al., 2014). In the case of mercury ions, the optimum potential of recovery was attained at 0.75 M thiourea. Hence, 0.5 M HCl and 0.75 M thiourea were applied to study the next parameter.

3.1.6. Flow rates of feed and strippant solutions

Flow rates of feed and strippant solutions ranging from 8.3×10^{-4} to 6.67×10^{-3} L·s^{-1} were evaluated to maximize the removal of arsenic and mercury ions. As seen in Fig. 8, at flow rates ranging from 8.3×10^{-4} to 1.67×10^{-3} L·s^{-1}, both extraction and recovery of arsenic and mercury ions remained unchanged at around 100 %. At 1.67×10^{-3} L·s^{-1}, the concentrations of arsenic and mercury ions in the outlet feed solution proved to be less than 0.02 and 0.001 mg·L^{-1}, thereby meeting the wastewater discharge standard set by Thailand's Ministry of Industry and Ministry of Natural Resources and Environment. As a result of shorter residence time, extraction and recovery of metal ions declined when the flow rates were higher
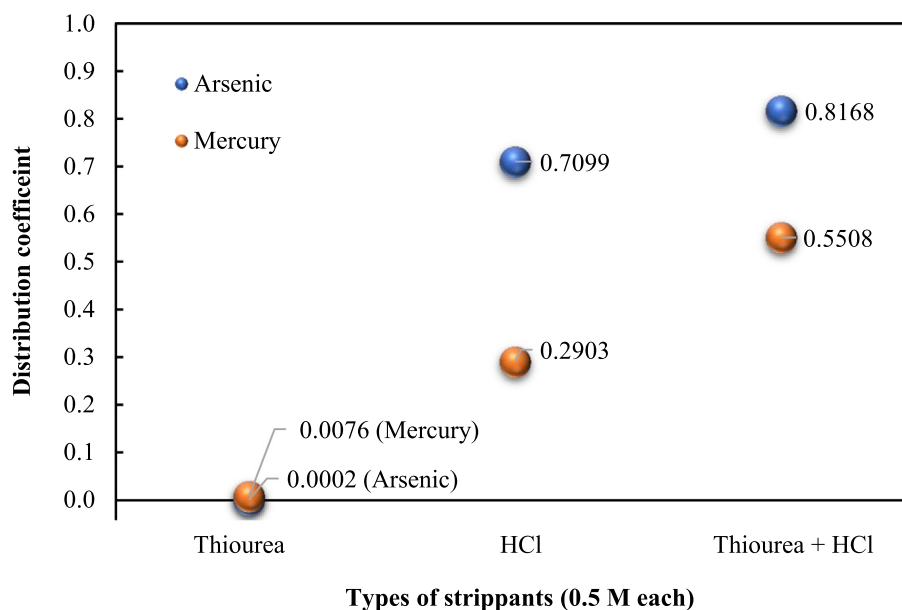

Fig. 5 Efficiency of recovery of arsenic and mercury ions using various types of strippant solutions (0.5 M each): [Aliquat 336] = 0.88 M, pH of feed solution = 11, flow rate of feed and strippant solutions = 1.67×10^{-3} L·s^{-1}, and operation time = 600 s.

Fig. 6 Distribution coefficients of recovery of arsenic and mercury ions utilizing different strippant solutions: extractant = 0.88 M Aliquat 336.

than 1.67×10^{-3} L·s^{-1}. Hence, flow rates of feed and strippant solutions of 1.67×10^{-3} L·s^{-1} were applied to maximize the recovery of arsenic and mercury ions.

3.1.7. Stability of the HFSLM system

The stability of the HFSLM system for the removal of arsenic and mercury ions was determined by testing the efficiency of extraction and recovery versus time. Thus, stability of the system was tested utilizing the optimum conditions: 0.88 M Aliquat 336 as the extractant, pH of feed solution of 11, the mixture of 0.5 M HCl and 0.75 M thiourea as the strippant solution, and flow rates of feed and stripping solutions of 1.67×10^{-3} L·s^{-1}. In Fig. 9, results are shown. It is noted that both extraction and recovery of arsenic and mercury ions remained constant at around 100 % during 18×10^{3} s of operation, indicating the stability of the liquid membrane in the HFSLM. Such an outcome also indicated that the system is at a steady state condition. For further studies, using a pilot plant, an investigation into the stability of the HFSLM system undertaking a longer time is recommended.

### 3.2. Intermolecular and intramolecular mechanisms of extraction and stripping

3.2.1. Density functional theory (DFT) calculation approach

Density functional theory is introduced in this work to analyze the extraction and stripping process of arsenic as well as mercury ions. Its calculation principle is provided in Appendix A. Initially, three-dimensional geometries in each reaction mechanism were constructed in cartesian coordinates. Geometry optimizations were carried out regarding the initial geometries by DFT calculations using B3LYP functionals with the LANL2DZ effective core potential double zeta valence basis set. Optimized structures were implemented using Hessian calculations to verify the structures that are located at the local minimum of the potential energy surface (PES) with no imag-

inary frequencies. The effect of solvent was considered by adding a conductor-like polarizable continuum (CPCM) solvation model in the standard state. Calculated thermodynamics data were attained using the information of frequency calculations. All these calculations were completed using the Gaussian09 program package and the molecular geometries were drawn using the Gabedit program package (Allouche, 2011). The results of analyzing mechanisms of extraction and stripping of arsenic and mercury ions using DFT are described in sections 3.2.2 and 3.2.3.

3.2.2. Reaction mechanisms as well as intermolecular and intramolecular properties for the separation of arsenic ions

3.2.2.1. Extraction of arsenic ions. In this research, H_3AsO_4 was used to prepare the synthetic feed solution. Moreover, the pH of the feed solution was adjusted to 11 whereby H_3AsO_4 was predominantly transformed into $HAsO_4^{2-}$ (Wilson et al., 2004). Therefore, the extraction reaction of arsenic ions using Aliquat 336 ($CH_3R_3N^+Cl^-$) is proposed as in Eq. (4) (Bey et al., 2010):

$$2(C_{25}H_{54}N^+)Cl^- + HAsO_4^{2-} \rightleftharpoons \overline{(C_{25}H_{54}N^+)_2 \cdot (HAsO_4^{2-})} + 2Cl^- \tag{4}$$
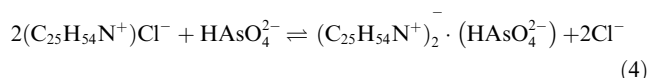
The overbar in Eq. (4) refers to the arsenic–carrier complex species in the liquid membrane phase.

According to DFT calculations, the mechanism of arsenic extraction can be described as follows. A molecule of $HAsO_4^{2-}$ reacts with 2 molecules of $(C_{25}H_{54}N^+)Cl^-$, resulting in the supramolecular complex $(C_{25}H_{54}N)_2 \cdot (HAsO_4)$. The tetrahedral optimized molecular structure of $HAsO_4^{2-}$ reveals that the lengths of the bond between As and oxygen atoms are 1.72, 1.73, 1.73, 1.88 Å and the O—H bond length is 0.98 Å. The bond angle between O-As-O is approximately 115° and the As—O—H bond angle is around 114°. In Fig. 10, the $(C_{25}H_{54}N^+)Cl^-$ optimized structure is shown. In
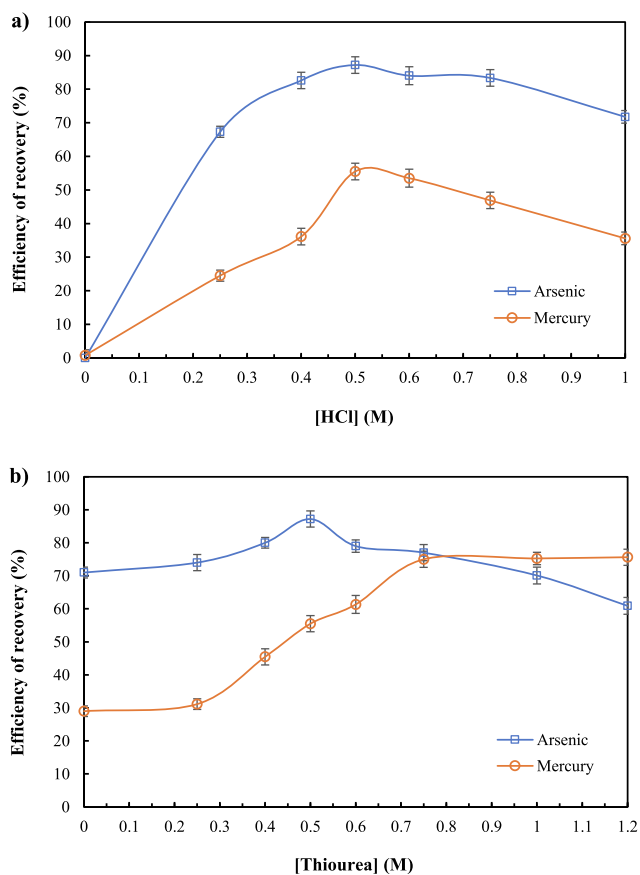
a)

b)

Fig. 7 Efficiency of recovery of arsenic and mercury ions utilizing 0.88 M Aliquat 336 as the extractant, pH of feed solution = 11, flow rate of feed and strippant solutions = 1.67×10^{-3} L·s^{-1}, and operation time = 600 s: a) 0.5 M thiourea mixed with HCl at various concentration, and b) 0.5 M HCl mixed with thiourea at various concentrations.
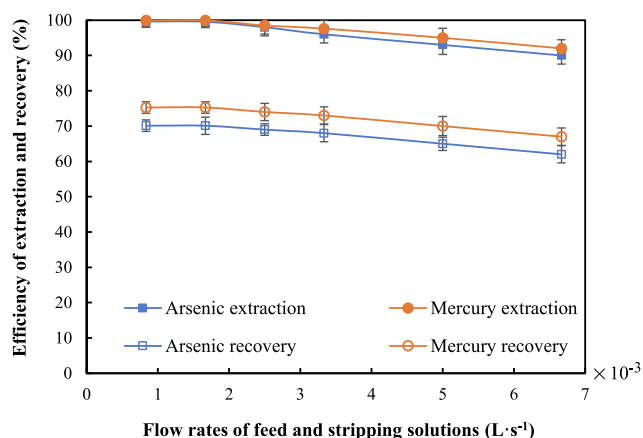

Fig. 8 Efficiency of recovery of arsenic and mercury ions at various flow rates of feed and strippant solutions, using 0.88 M Aliquat 336 as the extractant, pH of feed solution = 11, the mixture of 0.5 M HCl and 0.75 M thiourea as the strippant solution, and operation time = 600 s.
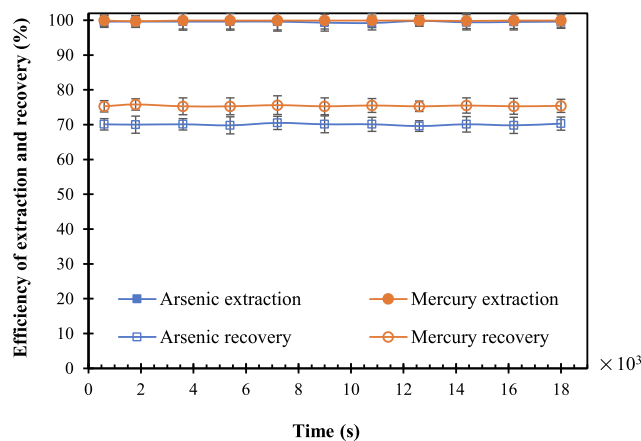

Fig. 9 Efficiency of recovery of arsenic and mercury ions versus time, using 0.88 M Aliquat 336 as the extractant, pH of feed solution = 11, the mixture of 0.5 M HCl and 0.75 M thiourea as the strippant solution, and flow rate of feed and strippant solutions = 1.67×10^{-3} L·s^{-1}.

the molecular formation, the electrostatic interaction between the opposite charge of $C_{25}H_{54}N^+$ and Cl$^-$ is dominant. Thus, when two molecules of $(C_{25}H_{54}N^+)$Cl$^-$ react with one molecule of $HAsO_4^{2-}$ in the extraction process, they lose two chloride anions and form a new supramolecular complex $(C_{25}H_{54}N)_2$·$(HAsO_4)$ via the coulombic (electrostatic) interaction between the opposite charge of $C_{25}H_{54}N^+$ and $HAsO_4^{2-}$. Two species of $C_{25}H_{54}N^+$ catch $HAsO_4^{2-}$ on the site opposite by pointing methyl groups to the oxygen atoms with an inter-distance of around 1.7 Å. Results show that the coulombic (electrostatic) interaction plays an important role in the reaction mechanism of $HAsO_4^{2-}$ extraction. The calculated thermodynamics properties reveal that this reaction is endothermic having a standard enthalpy change of 1.37×10^5 J·mol^{-1} and Gibbs free energy change of 3.99×10^5 J·mol^{-1}, respectively.

3.2.2.2. The synergistic stripping of arsenic from the supramolecular complex species. A mixture of thiourea $(CS(NH_2)_2)$ and hydrochloric acid was used as the synergistic strippant solution to enhance the efficiency of recovery of arsenic from the supramolecular complex $(C_{25}H_{54}N)_2$·$(HAsO_4)$. In Eq. (5) and Fig. 11, the reaction is shown. HCl and thiourea attack $HAsO_4^{2-}$ of the supramolecular complex $(C_{25}H_{54}N)_2$·$(HAsO_4)$. This reaction gives rise to a bond forming between the protons of the HCl and the oxygen atoms, yielding H_3AsO_4 and Cl$^-$ and results in the hydrogen bond between thiourea and H_3AsO_4, yielding the complex H_3AsO_4·$CS(NH_2)_2$. In the complex H_3AsO_4·$CS(NH_2)_2$, it is seen that an intramolecular hydrogen bond and chalcogen bond occurred, making the molecules more stable. Besides, the chloride anions, resulting from the breaking of the H-Cl bond, formed a coulombic attraction with two $C_{25}H_{54}N^+$, generating two $(C_{25}H_{54}N^+)$ Cl$^-$ molecules. The synergistic stripping process, using HCl and thiourea, proved to be exothermic with standard enthalpy change of -4.36×10^5 J·mol^{-1} and Gibbs free energy change of -5.94×10^5 J·mol^{-1}
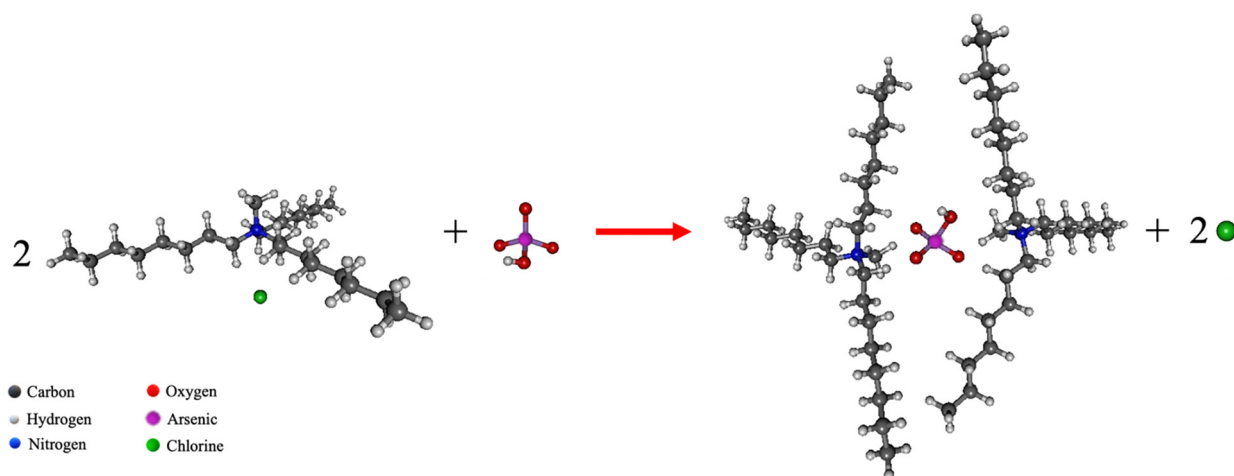
Fig. 10 The reaction of $(C_{25}H_{54}N^+)Cl^-$ and $(HAsO_4)^{2-}$ at B3LYP/LANL2DZ level of theory.
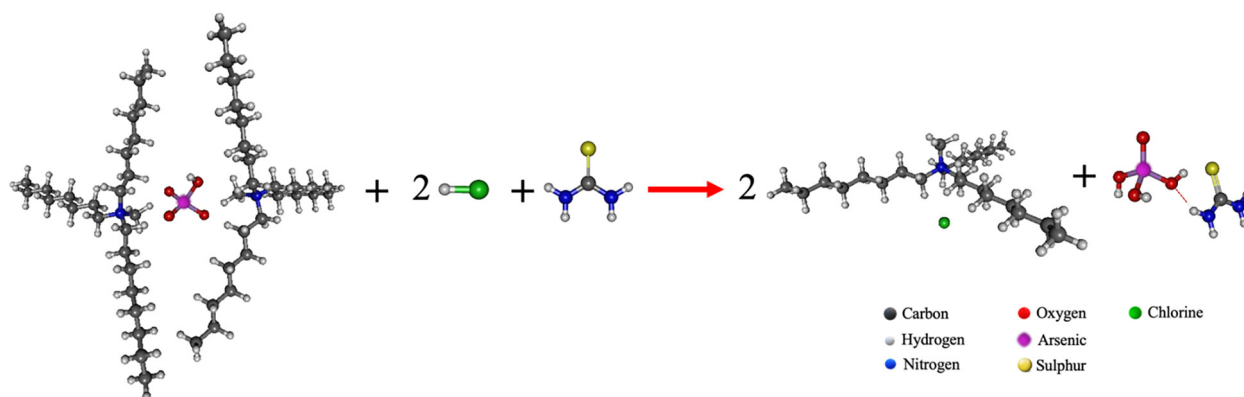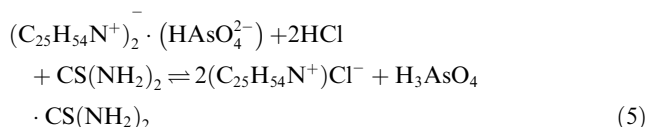

Fig. 11 The reaction of arsenic stripping using the mixture of thiourea and hydrochloric acid as the synergistic stripping solution at B3LYP/LANL2DZ level of theory.

$$(C_{25}H_{54}N^+)_2 \cdot \overline{(HAsO_4^{2-})} + 2HCl \\ + CS(NH_2)_2 \rightleftharpoons 2(C_{25}H_{54}N^+)Cl^- + H_3AsO_4 \\ \cdot CS(NH_2)_2 \qquad (5)$$

3.2.3. Reaction mechanisms as well as intermolecular and intramolecular properties for the separation of mercury ions

3.2.3.1. Extraction of mercury ions.
Aliquat 336, $(C_{25}H_{54}N^+)$ Cl^-, was used to extract mercury ions, which exist in the form of $HgCl_2$ in the aqueous solution. The extraction reaction of mercury ions using $(CH_3R_3N^+)Cl^-$ is proposed in this study, as shown in Eq. (6) (Fábrega and Mansur, 2007) and Fig. 12. According to DFT calculations, the lengths of the two bonds between the mercury and chloride anions are 2.60 Å with a bond angle of Cl-Hg-Cl 180.0°. When $(C_{25}H_{54}N^+)Cl^-$ reacts with $HgCl_2$, the $HgCl_2$ molecule forms a covalent bond with a chloride anion establishing a trigonal planar structure of $HgCl_3^-$. The coulombic (electrostatic) interaction between the opposite charge of $C_{25}H_{54}N^+$ and $HgCl_3^-$ attracts these two molecules creating a new supramolecular complex $(C_{25}H_{54}N^+) \cdot (HgCl_3^-)$. As shown in Fig. 12, $HgCl_3^-$ points two chloride anions to the $C_{25}H_{54}N^+$. The standard enthalpy change of this reaction is found to be -1.01×10^5 J·mol^{-1} and the standard Gibb free energy change is 4.62×10^5 J·mol^{-1}.

$$HgCl_2 + (C_{25}H_{54}N^+)Cl^- \rightleftharpoons \overline{(C_{25}H_{54}N^+) \cdot (HgCl_3^-)} \qquad (6)$$

The overbar in Eq. (6) stands for the mercury–carrier complex species in the liquid membrane phase.

3.2.3.2. Synergistic stripping of mercury from supramolecular complex species.
A mixture of HCl and thiourea, as the synergistic strippant solution, was used to strip the mercury complex species. In Eq. (7) and Fig. 13, the reaction mechanism is presented. The chloride anion of HCl attacks the position of $C_{25}H_{54}N^+$ and the proton of HCl forms a covalent bond with one chloride anion in $HgCl_3^-$. This reaction is followed by the attraction of thiourea by the halogen bonding, resulting in the products: $(C_{25}H_{54}N^+)Cl^-$ and $H^+ \cdot (HgCl_3)^- \cdot CS(NH_2)_2$. As shown in Fig. 13, it is seen that the intramolecular halogen bonding (2.35 Å) occurred inside the $H^+ \cdot (HgCl_3)^- \cdot CS(NH_2)_2$ molecule. This synergistic stripping reaction proved to be endothermic, yielding the standard enthalpy change of 2.0×10^5 J·mol^{-1} and the standard Gibbs free energy change of 2.34×10^5 J·mol^{-1}
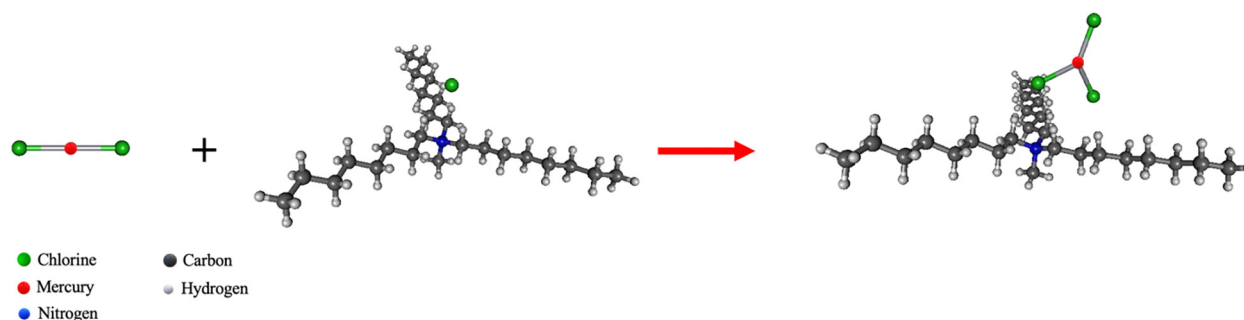
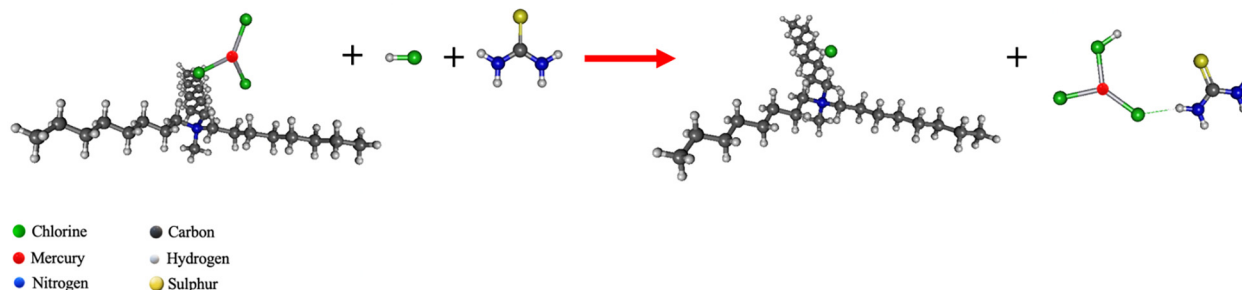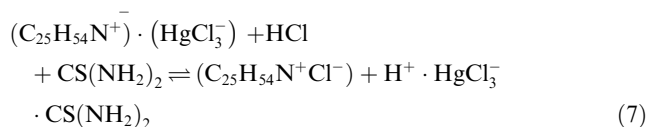**Fig. 12** The reaction of HgCl$_2$ extraction at B3LYP/LANL2DZ level of theory.

Fig. 13 The synergistic stripping reaction of mercury by the mixture of hydrochloric acid and thiourea at B3LYP/LANL2DZ level of theory.

$$(C_{25}H_{54}N^+) \cdot (HgCl_3^-) + HCl$$
$$+ CS(NH_2)_2 \rightleftharpoons (C_{25}H_{54}N^+Cl^-) + H^+ \cdot HgCl_3^-$$
$$\cdot CS(NH_2)_2 \tag{7}$$

3.3. Kinetics of extraction and recovery

To determine reaction rate constants and reaction orders of metal extraction and recovery, both integration and graphical approaches plotting the integral concentration of metal ions against time were applied. In Table 2, the results are depicted. In Fig. 14(a)-(d), the best fit is given. As a result of the highest R^2, reactions for the extraction and recovery of arsenic and mercury ions proved to be of second-order.

Consequently, the reaction rate constants of extraction and recovery of arsenic ions were 4.57×10^{-3} and 2.46×10^{-4} L·mg^{-1}·s^{-1}, respectively. Those of extraction and recovery of mercury ions proved to be 4.55 and 9.9×10^{-4} L·mg^{-1}·s^{-1}, respectively. These outcomes suggest that the rates of extraction for both arsenic and mercury ions are faster than those of recovery. In addition, the rate of extraction of mercury ions is seen to be much faster than that of arsenic ions.

3.4. Developing a mathematical model to describe mass transport mechanism and forecast the extractability of arsenic and mercury ions across HFSLM

Fig. 15(a) depicts the schema of transport of arsenic and mercury ions from the feed phase across the liquid membrane to

Table 2 Reaction orders (m/n) and reaction rate constants of extraction and recovery of arsenic and mercury ions (k_{Ex} and k_S).

m/n	Reaction	Plot	Arsenic ions		Mercury ions	
			Rate constant	R^2	Rate constant	R^2
1	Extraction	$\ln \frac{C_{M,0}}{C_M}$ versus t	1.50×10^{-2} s^{-1}	0.9333	5.58×10^{-2} s^{-1}	0.8344
	Stripping	$\ln \frac{C_{M,Org}}{C_{M,Org}-C_{M,S}}$ versus t	1.16×10^{-3} s^{-1}	0.9361	1.37×10^{-3} s^{-1}	0.9079
2	Extraction	$\frac{1}{C_M} - \frac{1}{C_{M,0}}$ and t	$\underline{4.57 \times 10^{-3}}$ L·mg^{-1}·s^{-1}	0.9822	$\underline{4.55}$ L·mg^{-1}·s^{-1}	0.9781
	Stripping	$\frac{1}{C_{M,Org}-C_{M,S}} - \frac{1}{C_{M,Org}}$ versus t	$\underline{2.46 \times 10^{-4}}$ L·mg^{-1}·s^{-1}	0.9904	$\underline{9.90 \times 10^{-4}}$ L·mg^{-1}·s^{-1}	0.9834
3	Extraction	$\frac{1}{2C_M^2} - \frac{1}{2C_{M,0}^2}$ and t	1.95×10^{-3} L^2·mg^{-2}·s^{-1}	0.9689	1.58×10^3 L^2·mg^{-2}·s^{-1}	0.9375
	Stripping	$\frac{1}{2(C_{M,Org}-C_M,S)^2} - \frac{1}{2C_{M,Org}^2}$ versus t	5.90×10^{-5} L^2·mg^{-2}·s^{-1}	0.9884	8.37×10^{-4} L^2·mg^{-2}·s^{-1}	0.9812

C_M, concentration of metal ions in the feed solution at time t; $C_{M,0}$, concentration of metal ions in the inlet feed solution; $C_{M,Org}$, initial concentration of metal ions in the organic carrier; $C_{M,S}$, concentration of metal ions in the stripping solution at time t.
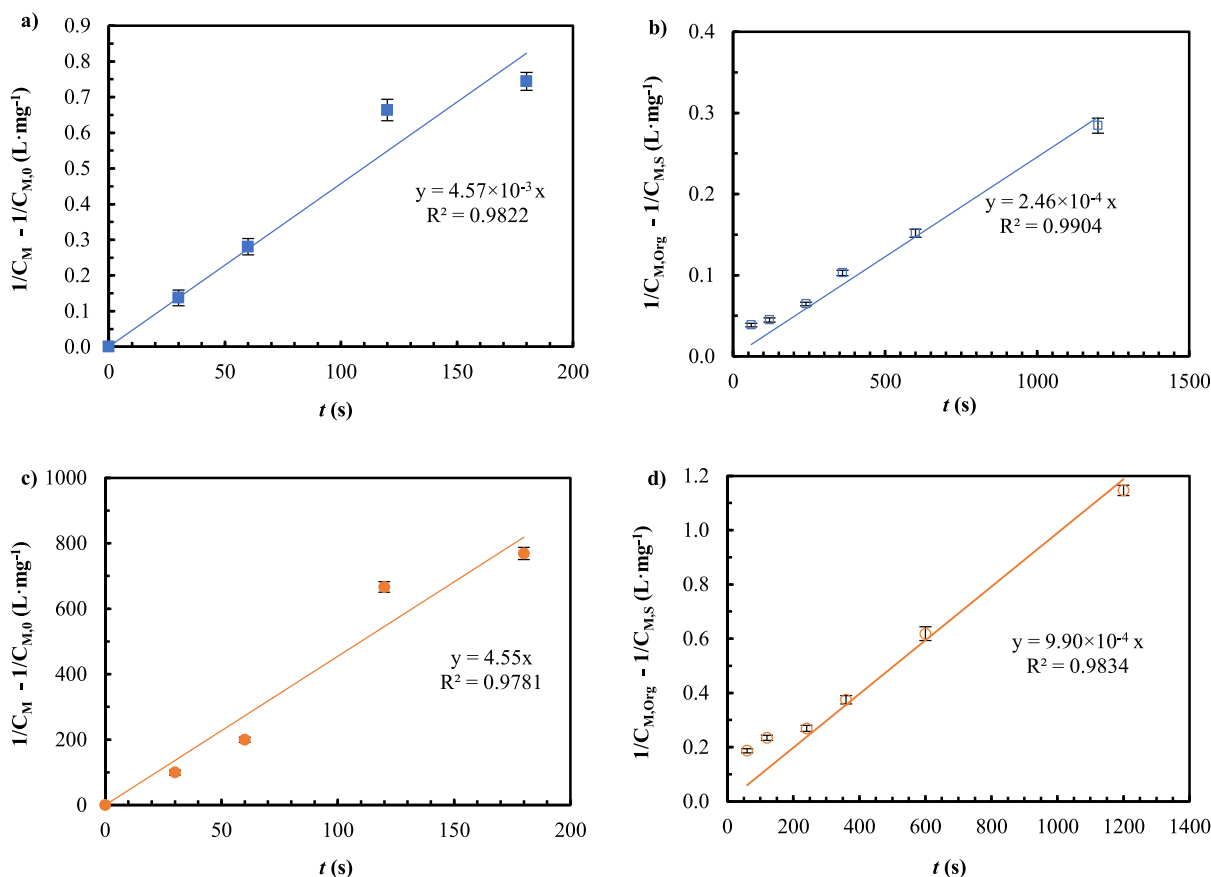
Fig. 14 The integral concentration of metal ions versus time: a) extraction of arsenic ions, b) recovery of arsenic ions, c) extraction of mercury ions and d) recovery of mercury ions.

the stripping phase. At the interface of feed and liquid membrane, arsenic and mercury ions in the feed phase combined with the organic carrier molecule(s) to create a supramolecular complex species of metal–carrier. According to the concentration gradient, the supramolecular complex species diffused across the liquid membrane phase to the interface of the liquid membrane and stripping, and then reacted with the strippant in the stripping solution. As a result, target metal ions were released into the stripping phase, whilst the carrier molecule, which was released from the supramolecular complex species, diffused backward to the interface of feed and liquid membrane and reacted with the target metal ions from the feed phase once more. Thus, arsenic and mercury ions can be extracted and recovered in a single-step operation.

The supramolecular complex species of the metal-carrier, occurring at the feed–liquid-membrane interface, diffused to the liquid-membrane–stripping interface and was recovered continuously by the strippant in the stripping phase. The total reactions, therefore, of arsenic and mercury extraction in Eqs. (4) and (6) can be considered as forward reaction. Their reaction rate can be expressed as follows:

$$r_{A,Ex}(x) = -k_{Ex}C_{A,F}^m(x) \qquad (8)$$

where $\times$ is the longitudinal axis of the hollow fiber in the feed phase (dm), k_{Ex} is the reaction rate constant of extraction (L·mg^{-1}·s^{-1}), $C_{A,F}$ is the concentration of metal ions in the feed phase (mg·L^{-1}) and m is the reaction order of extraction (-).

The model proposed in this study is considered at a steady state condition and created from the conservation of mass of metal ions in each increment (Δx) of the hollow fibers (Fig. 15(b)). Factors involved in the model comprise axial convection and extraction reaction at the feed–membrane interface; diffusion is neglected. The hypotheses of the model are:

1. Physical properties of the feed-phase i.e. temperature, pressure, and volume are all constant.
2. The inside diameter of the hollow fiber is extremely small. As a result, the concentration profiles of metal ions in the radial direction are constant, implying that the ion diffusion fluxes in the feed phase occur only in the axial direction.
3. Only the supramolecular complex species of the metal-carrier, produced by the extraction reaction, not metal ions, can transport into the liquid membrane phase.
4. Extraction reaction at the feed–liquid–membrane interface limits the rate of metal ion transport from the feed phase to the liquid membrane phase.
5. The supramolecular complex species of the metal-carrier, occurring at the feed–liquid-membrane interface, diffuses to the liquid-membrane–stripping interface and is recovered continuously by the strippant in the stripping phase. Therefore, the total reaction of metal extraction can be considered as forward reaction.
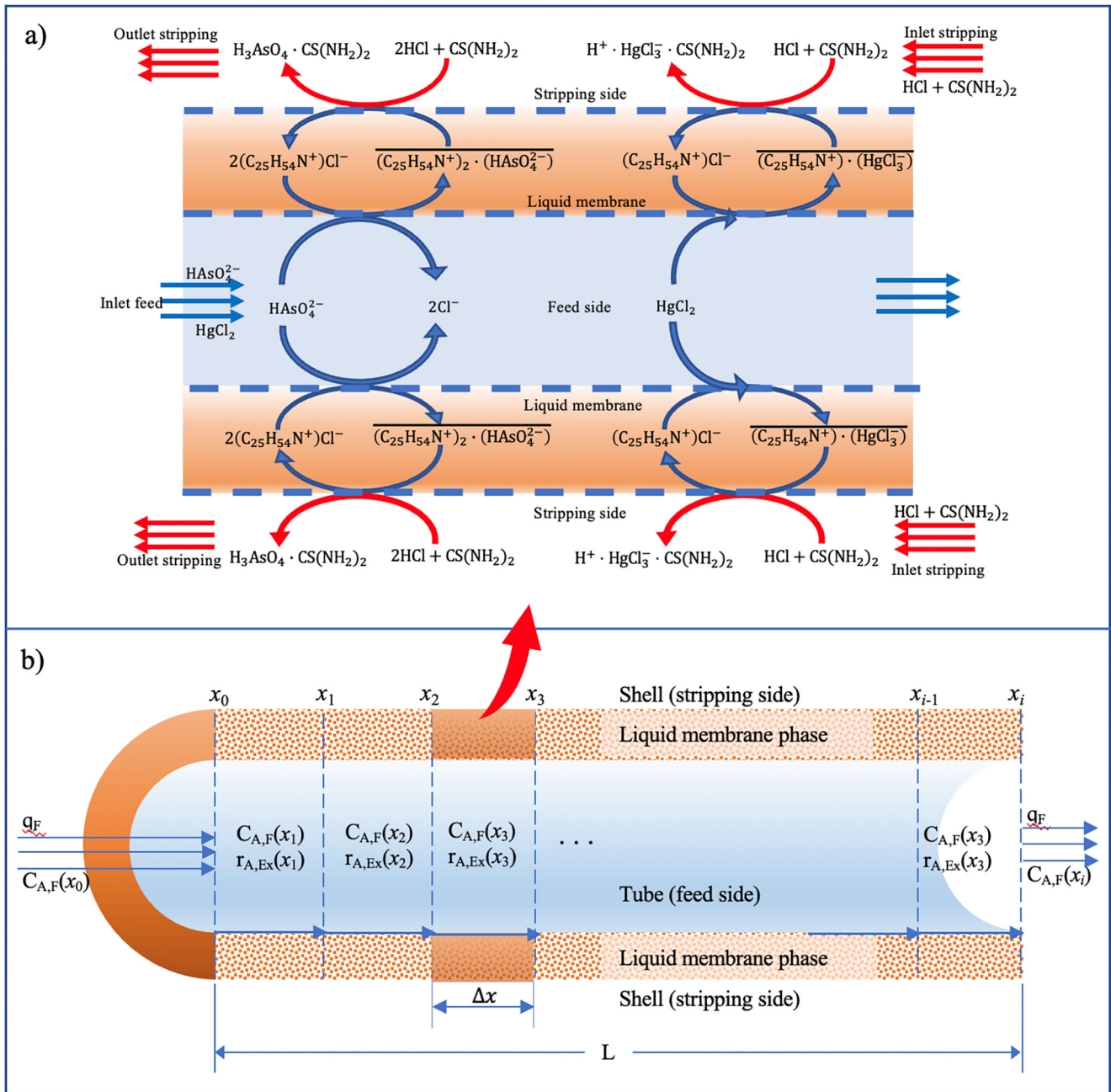
Fig. 15 Schema of arsenic and mercury ions transport across HFSLM: (a) mechanism of removal using Aliquat 336 as the carrier and HCl as the strippant, (b) mechanism of removal using Aliquat 336 as the carrier and the HCl/thiourea mixture as the strippant and (c) increment of a hollow fiber.

Conservation of mass of metal ions in each increment of a hollow fiber is given in Eq. (9):

[Rate of mass transport into the hollow fiber due to convection] –
[Rate of mass transport out of the hollow fiber due to convection] +
[Rate of mass extracted due to extraction reaction] =

[Rate of mass accumulation within the the hollow fiber]

$$(9)$$

Eq. (9) can be expressed as:

$$q_F C_{A,F}(x_{i-1}) - q_F C_{A,F}(x_i) + r_{A,Ex}(x_i) V_F = V_F \frac{dC_{A,F}(x_i)}{dt} \qquad (10)$$
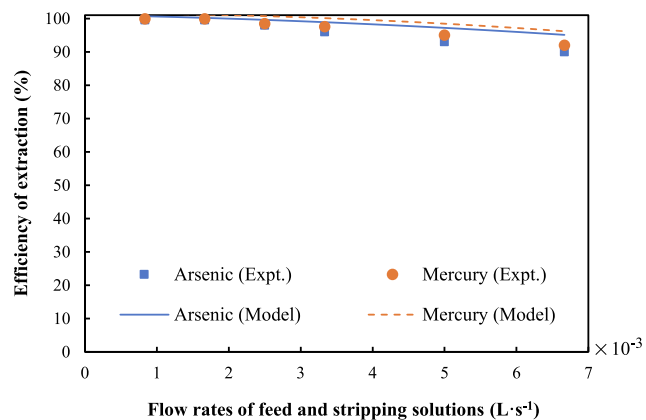
Fig. 16 Validation of the mathematical model using the experimental data.

where q_F refers to the volumetric flow rate of the aqueous feed solution (L·s^{-1}), $C_{A,F}$ denotes the concentration of metal ions in the feed phase (mg·L^{-1}), i represents the number of increments, $r_{A,Ex}$ stands for the rate of extraction reaction, and V_F refers to the volume of an increment of the hollow fiber (L): $V_F = \pi r_i^2 \Delta x; \Delta x = \frac{L}{i}$.

At steady state, the rate of mass accumulation is constant where $dC_{A,F}(x_i) / dt = 0$. Therefore, Eq. (10) becomes:

$$q_F C_{A,F}(x_{i-1}) - q_F C_{A,F}(x_i) + r_{A,Ex}(x_i)V_F = 0 \qquad (11)$$

Eq. (11) can be solved using the concept of Generating Function (as described in Appendix B) and yields Eq. (12), which is utilized to forecast the concentration of metal ions in the outlet feed solution viz. $C_{A,F}(x_i)$ measured in mg·L^{-1}:

$$\mathscr{C}_{A,F}(x_i) = \mathscr{C}_{A,F}(x_0)\left(\frac{1}{\lambda}\right)^i - \frac{\alpha V_F}{q_F}\sum_{k=1}^{i}\frac{1}{\lambda^{i-k+1}} \qquad (12)$$

The accuracy of the mathematical model for forecasting the extraction of metal ions via HFSLM can be determined by the average relative deviation (ARD):

$$\%ARD = \frac{1}{N}\sum_{i=1}^{N}\left|\frac{C_{Expt.} - C_{Model}}{C_{Expt.}}\right| \times 100 \qquad (13)$$

where $C_{Expt.}$ and C_{Model} are the concentrations of metal ions (mg·L^{-1}) attained from the experiment and the model, respectively. N is the number of observations.

The mathematical model developed, as in Eq. (12), was validated using the experimental data at various flow rates of feed and strippant solutions. In Fig. 16, the results of validation are depicted. Outcomes demonstrate that the extraction of arsenic and mercury ions estimated using Eq. (12) was in line with the experimental data, attaining average relative deviations of 5 %. These values confirmed that the chemical reaction at the interface of feed and liquid membrane is the predominant factor controlling the rate of arsenic and mercury ions transport from feed to the liquid membrane; diffusion of arsenic and mercury ions is negligible. It can be seen that the percentages of extraction of arsenic and mercury ions obtained from the experiment were slightly lower than those obtained from the prediction. Such an outcome occurred because the model neglected the effect of diffusion at the interface. However,

the model developed is still acceptable as the average relative deviation of prediction is as small as 5 %.

4. Conclusion

In this study, HFSLM proved to be effective for the simultaneous removal of arsenic and mercury ions from synthetic produced water. Percentages of extraction for both arsenic and mercury ions were found to be 100 % approximately. Meanwhile, the percentages of recovery for arsenic and mercury ions were 70 % and 75 %, respectively. Optimum removal was observed when using 0.88 M Aliquat 336 as the liquid membrane, pH of feed solution of 11, the mixture of 0.5 M HCl and 0.75 M thiourea as the strippant solution, and flow rates of both feed and strippant solutions of 1.67×10^{-3} L·s^{-1}. The quantum model based on DFT was applied to describe the mechanisms of extraction and recovery of arsenic and mercury ions. Moreover, the mathematical model based on the chemical reaction was consistent with the experimental data (%ARD = 5 %), indicating that the rate of reaction controls the rate of transport of arsenic and mercury ions from feed to the liquid membrane.

Competing interests

The authors declare no competing interests.

CRediT authorship contribution statement

Sira Suren: Conceptualization, Methodology, Formal analysis, Investigation, Writing – original draft. **Wikorn Punyain:** Software, Formal analysis. **Kreangkrai Maneeintr:** Resources. **Kasidit Nootong:** . **Ura Pancharoen:** Validation, Supervision.

Declaration of Competing Interest

The authors declare that they have no known competing financial interests or personal relationships that could have appeared to influence the work reported in this paper.

TEC) for providing computing resources contributing to the research results reported in this paper.

Appendix A:. Density functional theory (DFT) principle

The principle of DFT based on ground state electronic energy is a function of electron density: $\rho(r)$ measured in $e^-\cdot Å^{-3}$. Thus, electron density results from the square of the wave function (Jensen, 2007; Hohenberg and Kohn, 1964). The ground state electronic energy for the atoms and molecules can be written as follows:

$$E[\rho(r)] = T_{ni}[\rho(r)] + V_{ne}[\rho(r)] + V_{ee}[\rho(r)] + \Delta T[\rho(r)] \\ + \Delta V_{ee}[\rho(r)] \tag{A.1}$$

where $E[\rho(r)]$ is the total energy of all specific energy parts (J). $T_{ni}[\rho(r)]$ is the kinetic energy of the non-interacting electron (J). $V_{ne}[\rho(r)]$ is the nuclear-electron interaction energy (J). $V_{ee}[\rho(r)]$ is the classical electron–electron repulsion energy (J). $\Delta T[\rho(r)]$ is the correction to the kinetic energy (J). $\Delta V_{ee}[\rho(r)]$ is all non-classical correction to the electron–electron repulsion energy (J).

The calculations of the first three parts yield the exact solutions but the sum of the last two parts, the exchange–correlation energy, cannot be calculated to achieve the exact value. The total energy of all specific energy parts can be written as:

$$E[\rho(r)] = \sum_{i}^{N}(< \chi_i| -\frac{1}{2}\nabla_i^2|\chi_i > - < \chi_i| \sum_{k}^{nuclei} \frac{Z_k}{|r_i - r_k|}|\chi_i >) \\ + \sum_{i}^{N} < \chi_i|\frac{1}{2} \int \frac{\rho(r')}{|r_i - r'|}|\chi_i > + E_{XC}[\rho(r)] \tag{A.2}$$

where χ_i is the orbital used to minimize the total energy and can be calculated using the Kohn-Sham equation (1965), as shown below:

$$\varepsilon_i \chi_i = h_i^{KS} \chi_i \tag{A.3}$$

where h_i^{KS} is the Kohn-Sham one-electron operator:

$$h_i^{KS} = -\frac{1}{2}\nabla_i^2 - \sum_{k}^{nuclei} \frac{Z_k}{|r_i - r_k|} + \int \frac{\rho(r')}{|r_i - r'|}dr' + V_{XC} \tag{A.4}$$

where V_{XC} is a so-called functional derivative:

$$V_{XC} = \frac{\delta E_{XC}}{\delta \rho} \tag{A.5}$$

The exchange–correlation energy: $E_{XC}[\rho(r)]$ measured in J unit, can be calculated using the following equation:

$$E_{XC}[\rho(r)] = \int \rho(r)\varepsilon_{XC}[\rho(r)]dr \tag{A.6}$$

where ε_{XC} is the energy density (J·L^{-1}).

The exchange–correlation energy can be separated into two parts, as shown in Eq. (A.7). The first part is the exchange energy: $E_X[\rho(r)]$ measured in J unit. The second part is the electron–electron correlation energy: $E_C[\rho(r)]$ measured in J unit.

$$E_{XC}[\rho(r)] = E_X[\rho(r)] + E_C[\rho(r)] \tag{A.7}$$

B3LYP functional (Stephens et al., 1994) is the adiabatic connection method that describes the exchange–correlation energy, as follows:

$$E_{XC}^{B3LYP} = (1 - a)E_X^{LSDA} + aE_X^{HF} + b\Delta E_X^B + (1 - c)E_C^{LSDA} \\ + cE_C^{LYP} \tag{A.8}$$

where a, b, and c are equal to 0.20, 0.72, and 0.81, respectively.

Appendix B:. Details of solving the mathematical model

Conservation of mass of metal ions for each increment of a hollow fiber is as follows:

$$q_F C_{A,F}(x_{i-1}) - q_F C_{A,F}(x_i) + r_{A,Ex}(x_i)V_F = V_F \frac{dC_{A,F}(x_i)}{dt} \tag{B.1}$$

where q_F refers to the volumetric flow rate of the aqueous feed solution (L·s^{-1}). $C_{A,F}$ denotes the concentration of metal ions in the feed phase (mg·L^{-1}). i represents the number of increments (-). V_F refers to the volume of an increment in the hollow fiber (L): $V_F = \pi r_i^2 \Delta x$; $\Delta x = \frac{L}{i}$; $r_i$is the inside radius of hollow fiber (dm); Δx is the length of an increment of hollow fiber divided (dm); L is the effective length of hollow fiber (dm). $r_{A,Ex}$ stands for the rate of extraction reaction, which is expressed as in Eq (B.2):

$$r_{A,Ex}(x) = -k_{Ex}C_{A,F}^m(x) \tag{B.2}$$

where x is the longitudinal axis of the hollow fiber in the feed phase (dm), k_{Ex} is the reaction rate constant of extraction, $C_{A,F}$ is the concentration of metal ions in the feed phase (mg·L^{-1}) and m is the reaction order of extraction (-).

Linearizing Eq. (B.2) using the Taylor series yields:

$$r_{As,Ex}(x_i) = -[\beta C_{As,F}(x_i, t) + \propto] \tag{B.3}$$

where

$$\beta = mk_{Ex}C_{A,F}^{m-1}(x_0)$$

$$\propto = (1 - m)k_{Ex}C_{A,F}^m(x_0)$$

C_{A0} = the concentration of metal ions in the inlet feed solution (mg·L^{-1}).

At steady state, the rate of mass accumulation is constant where $dC_{A,F}(x_i) / dt = 0$. Therefore, Eq. (B.1) becomes:

$$q_F C_{A,F}(x_{i-1}) - q_F C_{A,F}(x_i) + r_{A,Ex}(x_i)V_F = 0 \tag{B.4}$$

Substituting Eq. (B.3) into Eq. (B.4) and rearranging the equation obtains:

$$C_{A,F}(x_{i-1}) - \left(1 + \frac{V_F\beta}{q_F}\right)C_{A,F}(x_i) - \frac{V_F\alpha}{q_F} = 0 \tag{B.5}$$

According to Eq. (B.5), the conservation of mass in increments 1, 2, 3, …, i can be expressed as:

$$C_{A,F}(x_0) - \left(1 + \frac{V_F\beta}{q_F}\right)C_{A,F}(x_1) - \frac{V_F\alpha}{q_F} = 0 \tag{B.6}$$

$$C_{A,F}(x_1) - \left(1 + \frac{V_F\beta}{q_F}\right)C_{A,F}(x_2) - \frac{V_F\alpha}{q_F} = 0 \tag{B.7}$$

$$C_{A,F}(x_2) - \left(1 + \frac{V_F\beta}{q_F}\right)C_{A,F}(x_3) - \frac{V_F\alpha}{q_F} = 0 \tag{B.8}$$

$$C_{A,F}(x_{i-1}) - \left(1 + \frac{V_F\beta}{q_F}\right)C_{A,F}(x_i) - \frac{V_F\alpha}{q_F} = 0 \tag{B.9}$$

The concept of the Generating Function is defined as:

$$\mathscr{C}_A(g) = \mathscr{C}_{A0}G^0 + \mathscr{C}_{A1}G^1 + \mathscr{C}_{A2}G^2 + \cdots \tag{B.10}$$

where G is a complex quantity.

Multiplying Eqs. (B.6) – (B.9) by $G^1, G^2, G^3, \ldots G^i$ and then summing them up achieves:

$$
\begin{aligned}
&G\left[C_A(x_0) + GC_A(x_1) + G^2 C_A(x_2) + \cdots\right] \\
&\quad - \lambda\left[C_A(x_0) + GC_A(x_1) + G^2 C_A(x_2) + G^3 C_A(x_3) + \cdots\right] \\
&\quad - \frac{v_p}{q_F}\alpha\left[G + G^2 + G^3 + \cdots\right] + \lambda C_A(x_0) \\
&= 0
\end{aligned}
\tag{B.11}
$$

$$\lambda = 1 + \frac{V_F \beta}{q_F}$$

Regarding the definition of the Generating Function, Eq. (B.11) can be represented as:

$$G\mathscr{C}_{A,F}(G) - \lambda\mathscr{C}_{A,F}(G) - \frac{V_F}{q_F}\alpha\sum_{j=1}^{i}G^j + \lambda\mathscr{C}_{A,F}(x_0) = 0 \tag{B.12}$$

Rearranging Eq. (B.12) yields:

$$\mathscr{C}_{A,F}(g) = \frac{\frac{V_F}{q_F}\alpha\sum_{j=1}^{i}G^j}{(G - \lambda)} - \frac{\lambda\mathscr{C}_{A,F}(0,0)}{(G - \lambda)} \tag{B.13}$$

By distributing the g function in Eq. (B.13) into polynomial form and taking the approach of undetermined coefficients, Eq. (B.14) is obtained, which is utilized to forecast the concentration of metal ions in the outlet feed solution viz. $C_{A,F}(x_i)$ measured in mg·L^{-1}:

$$\mathscr{C}_{A,F}(x_i) = \mathscr{C}_{A,F}(x_0)\left(\frac{1}{\lambda}\right)^i - \frac{\alpha V_F}{q_F}\sum_{k=1}^{i}\frac{1}{\lambda^{i-k+1}} \tag{B.14}$$

References

Allouche, A.R., 2011. Gabedit—A graphical user interface for computational chemistry softwares. J. Comput. Chem. 32 (1), 174–182.

Bai, B., Rao, D., Chang, T., Guo, Z., 2019. A nonlinear attachment-detachment model with adsorption hysteresis for suspension-colloidal transport in porous media. J. Hydrol. Reg. Stud 578,. https://doi.org/10.1016/j.jhydrol.2019.124080 124080.

Bey, S., Criscuoli, A., Figoli, A., Leopold, A., Simone, S., Benamor, M., Drioli, E., 2010. Removal of As(V) by PVDF hollow fibers membrane contactors using Aliquat-336 as extractant. Desalination. 264 (3), 193–200. https://doi.org/10.1016/j.desal.2010.09.027.

Chapman, T.W., 1997. Chapter 8, Extraction – Metals Processing. In: Rousseau, R.W. (Ed.), Handbook of Separation Process Technology. John Wiley & Sons Inc, Canada, pp. 467–499.

Chaturabul, S., Wongkaew, K., Pancharoen, U., 2012. Selective Transport of Palladium through a Hollow Fiber Supported Liquid Membrane and Prediction Model Based on Reaction Flux. Sep. Sci. Technol. 48. https://doi.org/10.1080/01496395.2012.673336.

Chaturabul, S., Srirachat, W., Wannachod, T., Ramakul, P., Pancharoen, U., Kheawhom, S., 2015. Separation of mercury (II) from petroleum produced water via hollow fiber supported liquid membrane and mass transfer modeling. J. Chem. Eng. 265, 34–46. https://doi.org/10.1016/j.cej.2014.12.034.

Choi, J.-W., Cho, K.S., Oh, B.-K., Youn, I.J., Jeong, J., Park, S., Lee, W.H., 2001. Numerical simulation of separation of cobalt and nickel using hollow fiber supported liquid membrane (HFSLM). J. Ind. Eng. Chem. 7 (4), 230–240.

Fábrega, F.d.M., Mansur, M.B., 2007. Liquid–liquid extraction of mercury (II) from hydrochloric acid solutions by Aliquat 336. Hydrometallurgy. 87(3), 83-90. doi: https://doi.org/10.1016/j.hydromet.2007.02.004.

Fontàs, C., Palet, C., Salvadó, V., Hidalgo, M., 2000. A hollow fiber supported liquid membrane based on Aliquat 336 as a carrier for rhodium(III) transport and preconcentration. J. Membr. Sci. 178 (1), 131–139. https://doi.org/10.1016/S0376-7388(00)00486-5.

Gallup, D.L., Strong, J.B., 2007. Removal of mercury and arsenic from produced water. Chevron Corporation, 1–9.

Ge, D., Yuan, H., Xiao, J., Zhu, N., 2019. Insight into the enhanced sludge dewaterability by tannic acid conditioning and pH regulation. Sci. Total Environ. 679, 298–306. https://doi.org/10.1016/j.scitotenv.2019.05.060.

Güell, R., Anticó, E., Salvadó, V., Fontàs, C., 2008. Efficient hollow fiber supported liquid membrane system for the removal and preconcentration of Cr (VI) at trace levels. Sep. Purif. Technol. 62 (2), 389–393.

Hohenberg, P., Kohn, W., 1964. Inhomogeneous electron gas. Phys. Rev. 136 (3B), B864.

Hu, X., Zhang, P., Wang, D., Jiang, J., Chen, X., Liu, Y., et al, 2021. AIEgens enabled ultrasensitive point-of-care test for multiple targets of food safety: Aflatoxin B1 and cyclopiazonic acid as an example. Biosens. Bioelectron. 182,. https://doi.org/10.1016/j.bios.2021.113188 113188.

Inbaraj, B.S., Wang, J., Lu, J., Siao, F., Chen, B., 2009. Adsorption of toxic mercury (II) by an extracellular biopolymer poly (γ-glutamic acid). Bioresour. Technol. 100 (1), 200–207.

Jantunen, N., Virolainen, S., Latostenmaa, P., Salminen, J., Haapalainen, M., Sainio, T., 2019. Removal and recovery of arsenic from concentrated sulfuric acid by solvent extraction. Hydrometallurgy. 187, 101–112. https://doi.org/10.1016/j.hydromet.2019.05.008.

Jensen, F., 2007. Introduction to Computational Chemistry. John Wiley & Son Ltd, West Sussex.

Kamran Haghighi, H., Irannajad, M., Fortuny, A., Sastre, A.M., 2019. Mathematical modeling on non-dispersive extraction of germanium from aqueous solutions using Aliquat 336. Water Sci. Technol. 78, 2489–2499. https://doi.org/10.2166/wst.2019.002.

Kandwal, P., Dixit, S., Mukhopadhyay, S., Mohapatra, P.K., 2011. Mass transport modeling of Cs(I) through hollow fiber supported liquid membrane containing calix-[4]-bis(2,3-naptho)-crown-6 as the mobile carrier. Chem. Eng. J. 174 (1), 110–116. https://doi.org/10.1016/j.cej.2011.08.057.

Kocherginsky, N., Yang, Q., Seelam, L., 2007. Recent advances in supported liquid membrane technology. Sep. Purif. Technol. 53 (2), 171–177.

Kohn, W., Sham, L.J., 1965. Self-consistent equations including exchange and correlation effects. Phys. Rev. 140 (4A), A1133. https://doi.org/10.1103/PhysRev.140.A1133.

Li, X.Y., Song, Y., Zhang, C.X., Zhao, C.X., He, C., 2021. Inverse CO2/C2H2 separation in a pillared-layer framework featuring a chlorine-modified channel by quadrupole-moment sieving. Sep. Purif. Technol. 279,. https://doi.org/10.1016/j.seppur.2021.119608 119608.

Lipnizki, F., 2010. Cross-flow membrane applications in the food industry. Membrane Technology: Membranes for food applications. 3, 1–24.

Liu, W., Li, J., Zheng, J., Song, Y., Shi, Z., Lin, Z., Chai, L., 2020. Different pathways for Cr (III) oxidation: implications for Cr (VI) reoccurrence in reduced chromite ore processing residue. Environ. Sci. Technol. 54 (19), 11971–11979. https://doi.org/10.1021/acs.est.0c01855.

Lothongkum, A.W., Suren, S., Chaturabul, S., Thamphiphit, N., Pancharoen, U., 2011. Simultaneous removal of arsenic and mercury from natural-gas-co-produced water from the Gulf of Thailand using synergistic extractant via HFSLM. J. Membr. Sci. 369 (1–2), 350–358.

Luo, F., Li, D., Wei, P., 2004. Synergistic extraction of zinc (II) and cadmium (II) with mixtures of primary amine N1923 and neutral organophosphorous derivatives. Hydrometallurgy. 73 (1–2), 31–40.

Ma, L., Zhao, Z., Dong, Y., Sun, X., 2018. A synergistic extraction strategy by Cyanex 572 and Cyanex923 for Th(IV) separation. Sep. Purif. Technol. 191, 307–313. https://doi.org/10.1016/j.seppur.2017.09.025.

Mishra, P.L., Swain, B., Pabby, A.K., Singh, M., Gulati, S., Ramasubramanium, S., 2021. Mathematical Modeling of Extraction of Neodymium using Pseudo-emulsion based Hollow Fiber Strip Dispersion (PEHFSD). Journal of Applied Membrane Science & Technology 25 (3), 63–79.

Mohdee, V., Parasuk, V., Pancharoen, U., 2021. Synergistic effect of Thiourea and HCl on Palladium (II) recovery: An investigation on Chemical structures and thermodynamic stability via DFT. Arabian J. Chem. 14, (7). https://doi.org/10.1016/j.arabjc.2021.103196 103196.

Nasim Rahnama, S., Aghaie, M., Noei, M., Aghaie, H., 2021. Theoretical study of the catalytic effect of TM-C_4H_4 and TM-C5H5 (TM = Cr, Ti, V, Sc) on the activation of O2 at the cathode and CH3OH at the anode in ''CH_3OH-O_2'' fuel cell via DFT computational method. Arabian J. Chem. 14, (4). https://doi.org/10.1016/j.arabjc.2021.103062 103062.

Neff, J.M., Rabalais, N.N., Boesch, D.F., 1987. Offshore oil and gas development activities potentially causing long-term environmental effects. Long-term environmental effects of offshore oil and gas development. Elsevier, London (UK), p. 149473..

Pajuelo, E., Rodríguez-Llorente, I.D., Dary, M., Palomares, A.J., 2008. Toxic effects of arsenic on Sinorhizobium-Medicago sativa symbiotic interaction. Environ. Pollut. 154 (2), 203–211.

Pancharoen, U., Poonkum, W., Lothongkum, A.W., 2009. Treatment of arsenic ions from produced water through hollow fiber supported liquid membrane. J. Alloys Compd. 328–334. https://doi.org/10.1016/j.jallcom.2009.04.006.

Pancharoen, U., Somboonpanya, S., Chaturabul, S., Lothongkum, A. W., 2010. Selective removal of mercury as $HgCl_4^{2-}$ from natural gas well produced water by TOA via HFSLM. J. Alloys Compd. 489 (1), 72–79.

Pancharoen, U., Wongsawa, T., Lothongkum, A.W., 2011. A Reaction Flux Model for Extraction of Cu(II) with LIX84I in HFSLM. Sep. Sci. Technol. 46 (14), 2183–2190. https://doi.org/10.1080/01496395.2011.595287.

Perez, M.E.M., Reyes-Aguilera, J.A., Saucedo, T.I., Gonzalez, M.P., Navarro, R., Avila-Rodriguez, M., 2007. Study of As(V) transfer through a supported liquid membrane impregnated with tri-octylphosphine oxide (Cyanex 921). J. Membr. Sci. 302 (1), 119–126. https://doi.org/10.1016/j.memsci.2007.06.037.

Rathore, N., Sonawane, J., Kumar, A., Venugopalan, A., Singh, R., Bajpai, D., Shukla, J., 2001. Hollow fiber supported liquid membrane: a novel technique for separation and recovery of plutonium from aqueous acidic wastes. J. Membr. Sci. 189 (1), 119–128.

San Román, M., Bringas, E., Ibanez, R., Ortiz, I., 2010. Liquid membrane technology: fundamentals and review of its applications. J. Chem. Technol. Biotechnol. 85 (1), 2–10.

Scott, M.D., Schorp, J., Sutherlin, L., Robertson, J.D., 2020. Isotope harvesting with hollow fiber supported liquid membrane (HFSLM). Appl. Radiat. Isot. 157, 109027.

Stephens, P.J., Devlin, F.J., Chabalowski, C.F., Frisch, M.J., 1994. Ab initio calculation of vibrational absorption and circular dichroism spectra using density functional force fields. J. Phys. Chem. 98 (45), 11623–11627.

Sun, X., Li, J., Sun, X., Zheng, J., Wu, Z., Liu, W., et al, 2021. Efficient stabilization of arsenic in the arsenic-bearing lime-ferrate sludge by zero valent iron-enhanced hydrothermal treatment. Chem. Eng. J. 421,. https://doi.org/10.1016/j.cej.2021.129683 129683.

Sunsandee, N., Kunthakudee, N., Chutvirasakul, B., Phatanasri, S., Ramakul, P., 2017. Enantioseparation of (S)-amlodipine from pharmaceutical wastewater by hollow-fiber supported liquid membrane: central composite design and optimization. Desalin. Water Treat. 72, 207–215.

Sunsandee, N., Phatanasri, S., Ramakul, P., Pancharoen, U., 2018. Thermodynamic parameters and isotherm application on enantiomeric separation of levofloxacin using hollow fiber supported liquid membrane system. Sep. Purif. Technol. 195, 377–387.

Thailand regulatory discharge standards, 1996. Ministry of Industry. Thailand.

Van der Vaart, R., Akkerhuis, J., Feron, P., Jansen, B., 2001. Removal of mercury from gas streams by oxidative membrane gas absorption. J. Membr. Sci. 187 (1–2), 151–157.

Van Mourik, T., Bühl, M., Gaigeot, M.-P., 2014. Density functional theory across chemistry, physics and biology. Phil. Trans.R.Soc. 372, 20120488. https://doi.org/10.1098/rsta.2012.0488.

Wannachod, T., Leepipatpiboon, N., Pancharoen, U., Nootong, K., 2014. Synergistic effect of various neutral donors in D2EHPA for selective neodymium separation from lanthanide series via HFSLM. J. Ind. Eng. Chem. 20, 4152–4162. https://doi.org/10.1016/j.jiec.2014.01.014.

Wilson, S.D., Kelly, W.R., Holm, T.R., Talbott, J.L., 2004. Arsenic removal in water treatment facilities: survey of geochemical factors and pilot plant experiments, Illinois State Water Survey, 2004.

Zhang, W., Cui, C., Hao, Z., 2010. Transport Study of Cu(II) Through Hollow Fiber Supported Liquid Membrane. Chin. J. Chem. Eng. 18 (1), 48–54. https://doi.org/10.1016/S1004-9541(08)60322-5.